

# Direct Control of Visual Perception with Phase-specific Modulation of Posterior Parietal Cortex

Andrew Jaegle<sup>1\*</sup> and Tony Ro<sup>1,2</sup>

## Abstract

■ We examined the causal relationship between the phase of alpha oscillations (9–12 Hz) and conscious visual perception using rhythmic TMS (rTMS) while simultaneously recording EEG activity. rTMS of posterior parietal cortex at an alpha frequency (10 Hz), but not occipital or sham rTMS, both entrained the phase of subsequent alpha oscillatory activity and produced a phase-dependent change on subsequent visual perception, with

lower discrimination accuracy for targets presented at one phase of the alpha oscillatory waveform than for targets presented at the opposite phase. By extrinsically manipulating the phase of alpha before stimulus presentation, we provide direct evidence that the neural circuitry in the parietal cortex involved with generating alpha oscillations plays a causal role in determining whether or not a visual stimulus is successfully perceived. ■

## INTRODUCTION

Neuronal oscillations in the alpha band (9–12 Hz) are one of the most prominent endogenous brain rhythms measured in human EEG, yet their precise function remains unknown (Başar, 2012; Başar & Güntekin, 2012; Klimesch, 2012; Mathewson et al., 2011; Jensen & Mazaheri, 2010; Lindsley, 1952; Adrian & Matthews, 1934; Berger, 1929). Alpha oscillations have been suggested to play a role in perception and attention, with decreases in alpha power and alpha coherence preceding expected and attended stimuli and predicting the success of detection (Capotosto, Babiloni, Romani, & Corbetta, 2009; Hanslmayr et al., 2007; Worden, Foxe, Wang, & Simpson, 2000; Varela, Toro, John, & Schwartz, 1981). Recently, studies have shown a correlation between the phase of the alpha oscillation at the time of stimulus presentation and successful visual perception, with near-threshold stimulus detection varying continuously from a maximum rate at one phase of the alpha waveform (270° on the alpha sinusoid) to a minimum rate at the opposite phase of alpha (90°; Dugué, Marque, & VanRullen, 2011; Mathewson, Gratton, Fabiani, Beck, & Ro, 2009). Other results suggest that these phase-correlated behavioral effects may reflect modulations in cortical excitability following the alpha phase, with peak excitability occurring at the phase opposite to minimum excitability, as measured by the fMRI BOLD response (Scheeringa, Mazaheri, Bojak, Norris, & Kleinschmidt, 2011) and TMS-induced phosphene production (Dugué et al., 2011; Romei et al., 2008). Similarly, the average firing rate of somato-

sensory neurons has been shown to vary with alpha phase, with the highest firing rates occurring at one phase of the alpha waveform and minimum firing rates at the opposite phase (Haegens, Nächer, Luna, Romo, & Jensen, 2011). Similar phase-specific effects have also been measured for lower oscillatory frequencies (Busch, Dubois, & VanRullen, 2009; Lakatos, Karmos, Mehta, Ulbert, & Schroeder, 2008).

In the current study, we entrained alpha oscillations with rhythmic TMS (rTMS) of the posterior parietal cortex at 10 Hz to assess whether the phase of these posterior alpha oscillations plays a causal role in visual perception. We targeted one of the purported generators of alpha located near the intraparietal sulcus (Thut & Miniussi, 2009). rTMS at this alpha frequency has been suggested to excite neuronal populations at the target site, rather than to disrupt or interfere with processing, as in other types of TMS (Bolognini & Ro, 2010). rTMS has accordingly become an important tool for directly modulating ongoing alpha power and phase (Thut, Miniussi, & Gross, 2012). rTMS at alpha frequencies suggests an important role for experimentally modulated alpha power in performance on memory tasks (Sauseng et al., 2009) and in setting the threshold for auditory tone discrimination (Weisz, Lüchinger, Thut, & Müller, 2012). Several studies have also used alpha-band transcranial direct current stimulation or transcranial alternating current stimulation to demonstrate a modulation of ongoing alpha power or phase in sensory/attentional networks (Neuling, Rach, Wagner, Wolters, & Herrmann, 2012; Zaehle, Rach, & Herrmann, 2010).

Crucially, several studies have demonstrated that rTMS bursts at frequencies within the alpha band over occipitoparietal areas can entrain ongoing alpha and can modulate the activity of visual and attentional networks in which

<sup>1</sup>The City University of New York Graduate Center, <sup>2</sup>The City College of the City University of New York

\*Current affiliation: University of Pennsylvania.

alpha is implicated (Thut et al., 2011; Klimesch, Sauseng, & Gerloff, 2003). Occipito-parietal rTMS in the alpha band (10 Hz), but not at other nearby frequencies (5 Hz or 20 Hz), has been demonstrated to lead to behavioral modulations that are consistent with a role of alpha-band modulation in attention and perception (Romei, Gross, & Thut, 2010). To assess whether alpha phase plays a direct role in visual perception, we experimentally induced an alpha oscillation at varying phases with respect to visual target onset. If alpha does have a direct effect on visual perception, then stimuli presented near one phase of the induced alpha waveform should be discriminated more accurately than those stimuli presented near the opposite phase.

## METHODS

### Participants

All methods and procedures were approved by the institutional review board of The City University of New York. Eleven participants were recruited from The City University of New York and participated in the study after informed consent. All participants had normal or corrected-to-normal vision, were free of neurological disorders, had no implanted devices, and had no family history of seizures or epilepsy. The data from two participants were excluded from analysis because their discrimination of both masked and unmasked targets was at ceiling (i.e., the target was not significantly masked). The data from two additional participants were excluded because masked target discrimination accuracy was at chance for one participant, and excessive EEG signal noise was present throughout the recording for the other participant. The data for the remaining seven participants (one woman, all right-handed) between the ages of 21 and 31 years (mean = 24.7 years) were included in the analyses.

### Stimuli and Behavioral Protocol

A PC with an Intel dual-core processor was used to record the EEG data. Another PC, also with an Intel dual-core processor, was used to trigger the TMS device and the EEG computer and for stimulus display and behavioral data acquisition. The PC used for stimulus presentation was connected to a 17-in. CRT monitor (Sony Trinitron Multiscan 220GS) with a refresh rate set at 100 Hz. Participants were seated 57 cm away from the monitor in a dark room with their chin positioned on a chin rest. Participants were asked to maintain central fixation throughout the experiment and to blink only after responding to a trial.

All stimuli used in the experiment were black ( $0 \text{ cd/m}^2$ ), displayed on a gray background ( $10.65 \text{ cd/m}^2$ ), and were presented at the center of the display. Each trial began with a 500-msec presentation of a small fixation cross (Figure 1). After fixation offset, a blank screen interval of 300 msec occurred, during which rTMS (three pulses, with an inter-pulse interval of 100 msec) was delivered on 75% of trials.

To control the phase of stimulus onset, a target stimulus (a square or diamond, each presented on 50% of the target-present trials and with an edge length of  $1.7^\circ$  of visual angle) was presented with equal probability after the 300-msec stimulation/no stimulation interval. The target was presented for 10 msec on two thirds of trials, whereas the remaining one thirds of the trials were catch trials in which no target was presented. The target was followed by a blank screen for 70 msec. A metacontrast mask was then presented for 20 msec on two thirds of trials, with the remaining one thirds of the trials being target-only/no mask trials. The mask consisted of a black circle (diameter of  $1.9^\circ$  of visual angle) with a central cutout area that was the same gray color as the screen background. The center cutout had the exact dimensions and on-screen position as the two superimposed target shapes. After mask presentation, the screen remained blank until the participant responded, after which the next trial commenced.

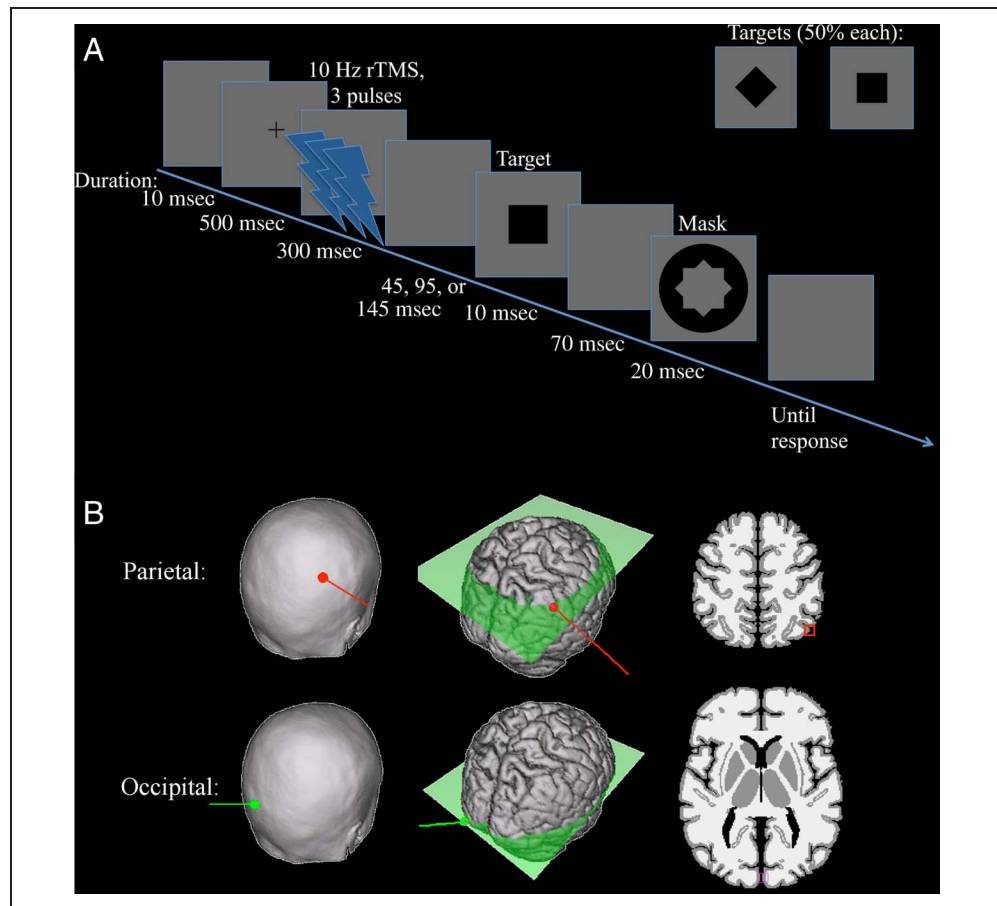
In a pilot experiment, the TMS discharge caused the stimulus display monitor raster to flicker. This flicker was clearly visible when the raster was drawing the background gray. To ensure that this flicker was not visible and did not affect performance on the task or alpha entrainment, we changed the display color on the top and bottom 1/10th of the screen to black. We synchronized each TMS discharge to the beginning of a raster cycle and verified that the flicker was invisible against the black display color. Consequently, the raster refresh cycle of 100 Hz was synchronized with rTMS discharge. As our stimuli were presented in the center of the screen, the onset of the center of each stimulus was physically one-half raster cycle (5 msec) before the times of interest for our analyses (i.e., 45, 95, and 145 msec post-TMS), but because the effects of the rTMS are not instantaneous and also for the sake of rounding, we henceforth refer to these SOAs as 50, 100, and 150 msec. Each target was displayed for a single raster cycle (10 msec), which corresponds to 1/10th of the duration of a single period of 10-Hz alpha. Thus, if the middle point of a stimulus presentation falls near one phase of the alpha waveform, the entire duration of the stimulus presentation falls in the same phase quadrant.

Participants made a forced-choice discrimination of the target identity by clicking the left mouse button to report a square and the right mouse button to report a diamond. Participants were informed that the identity of the stimulus would sometimes be very difficult to determine and that they should guess if unsure. They were also asked to respond as accurately and quickly as possible. Each participant completed three blocks of 144 trials, for a total of 432 trials. The presentations of all stimulus and interval conditions were randomized within a block.

### TMS

A MagStim Rapid stimulator (Carmarthenshire, UK) with two interchangeable 13.5-cm outer diameter circular coils was used. TMS position and intensity were set for each

**Figure 1.** Individual trial timeline with stimulus presentation durations and locations of rTMS. (A) Each trial began with a 500-msec presentation of a small fixation cross. After fixation offset, there was a blank screen interval of 300 msec, during which rTMS was delivered over the parietal cortex, occipital cortex, or with the coil held off the head (sham stimulation condition) at 10 Hz on 75% of trials. There was no stimulation on the remaining 25% of trials. To control the phase of stimulus onset, a target stimulus (a square or diamond with equal probability) was presented on two thirds of the trials at the three time points of interest after the stimulation/no stimulation interval. The target was followed by a blank screen for 70 msec and a metacontrast mask was then presented for 20 msec on 2/3 of trials. EEG was simultaneously recorded to measure the effects of the rTMS on alpha oscillatory activity. (B) rTMS at 10 Hz was targeted over the posterior parietal cortex in the right hemisphere (between P2, P4, CP2, and CP4 electrode positions; top row) or an occipital lobe site that when stimulated produced visual phosphenes (near Oz electrode position; bottom row).



individual participant by first applying single-TMS pulses at 50% of maximum stimulator output approximately 2.5 cm above the inion. With the participants' eyes closed, the position and intensity of the TMS coil were then adjusted until participants reported phosphenes. All adjustments were made in the experimental testing booth with the lights off and while the participant wore the EEG cap. The final coil position was within approximately 2 cm of the initial stimulation position. TMS coil placement fell along the midline or over the leftmost margin of the right hemisphere and corresponded to a position between POz and Oz on the standard 10/20 electrode placement system for all participants. This position was then maintained, and the intensity modified until the participant reported phosphenes in at least three of five consecutive TMS discharges. The mean TMS intensity used for this experiment was 58% of maximum output. After each experimental session, we asked the participant if they had experienced any difficulty distinguishing the target stimuli because of phosphenes or other TMS-related effects. Although some participants reported discomfort, no participants reported any difficulty discriminating targets from phosphenes.

Each participant completed three rTMS conditions: occipital, parietal, and sham rTMS. In each rTMS condition, each rTMS-present trial consisted of an identical sequence of three TMS pulses separated by 100 msec (10 Hz rTMS). These three rTMS conditions were presented in separate blocks, with the block order counter-balanced across participants. For the occipital rTMS condition, we positioned the TMS coil at the phosphene site. For the parietal rTMS condition, we positioned the TMS coil at the position between electrodes P2, P4, CP2, and CP4, corresponding to the average source of alpha generation, as previously reported (Thut et al., 2011). For the sham rTMS condition, we positioned the TMS coil centrally approximately 15 cm away from and behind the participant's occipital pole, and we oriented the front of the coil parallel to the surface of the skull.

## EEG

We simultaneously recorded continuous EEG during the main experiment. All EEG data were recorded using an ANT TMS-compatible EEG system and the ANT ASA-Lab

EEG software environment. All processing and analyses of EEG data were performed in MATLAB (Mathworks, Natick, MA) using the EEGLAB toolbox (Delorme & Makeig, 2004) and custom scripts. We recorded from 62 Ag/AgCl electrodes using a TMS-compatible electrode cap with a standard 10/20 layout and from five Ag/AgCl external electrodes. The electrodes were referenced on-line to an average reference of all electrodes and were subsequently re-referenced off-line to an average of the two external mastoid electrodes. Skin/electrode impedance for all electrodes was maintained below 10 k $\Omega$ .

All data were digitized and recorded at a sampling rate of 2048 Hz but were down-sampled to 256 Hz for analysis. Before analysis, a high-pass filter was applied to the data at 0.1 Hz to remove slow signal drifts using a two-way least squares finite impulse response (FIR) filter. All subsequent analyses were performed on data epoched from 500 msec before the rTMS train onset to 1000 msec after the end of rTMS, with the first 300 msec of each epoch serving as the epoch baseline. We manually rejected all epochs with eye blinks or excessive noise during the baseline, the rTMS interval, or stimulus presentation periods (83% acceptance rate). To eliminate the high-voltage artifacts associated with TMS, data from the interval between 10 msec before and 35 msec after each TMS pulse were linearly interpolated. Visual inspection of individual trials confirmed that the artifact was completely removed. The interpolated data were not included in any of the analyses.

Average alpha-band EEG waveforms were obtained by bandpass filtering the average response at an individual electrode (time-locked to the TMS pulses) using a two-way least squares FIR filter with low-edge and high-edge frequency cutoffs of 9 and 12 Hz, respectively. Measures of intertrial coherence (ITC) and estimates of instantaneous alpha phase were calculated using EEGLAB's built-in functions and custom MATLAB scripts. ITC is a measure of phase alignment of ongoing oscillations between trials on a continuous scale between 0 and 1, where 0 = *random phase alignment* and 1 = *perfect alignment*. We calculated ITC with a sinusoidal wavelet decomposition using a 0.5-cycle wavelet applied to overlapping Hanning-tapered time windows for each epoch after the artifact removal period. ITC and phase values were obtained at the frequency in the alpha range (9–12 Hz) with maximum coherence over the course of the experiment, as determined for each participant by EEGLAB (mean = 10.2 Hz). The plotted significance limits for the ITC were calculated by randomly shuffling single-trial data from the baseline period across all rTMS conditions.

## Statistics

All statistics were performed using custom scripts written in MATLAB. The ANOVA and subsequent two-tailed *t* tests of the behavioral data were conducted on normalized discrimination rates for the masked target trials with rTMS. We calculated normalized discrimination rates for

each participant at each SOA/rTMS condition using the following formula for each participant: (mean rate in an SOA/rTMS condition – mean rate in corresponding rTMS condition across SOAs)/(mean rate in corresponding rTMS condition across SOAs). The normalized discrimination rate for each participant is thus a measure of the change in that participant's performance in a particular SOA/rTMS condition relative to their overall performance on all trials with rTMS at that location.

Circular statistics were computed using the MATLAB CircStat toolbox (Philipp, 2009). All phase statistics were analyzed using the EEG data from electrode P2, which is the electrode closest to the source of the parietal alpha generator. Similar results for all tests were obtained at other occipito-parietal electrodes. For all EEG phase data analyses, rTMS-present trials were pooled across all target/mask and target SOA conditions.

## RESULTS

### Target Discrimination Performance

Participants discriminated unmasked targets at a mean rate of 97% and masked targets at a mean rate of 82%. Participants displayed a wide range of baseline discrimination rates (individual participants' mean discrimination rate on target present followed by mask trials ranged from 65% to 94%, mean = 82%, *SD* = 11%). Accordingly, for each rTMS site, we normalized the behavioral data to highlight the change in performance at particular times following rTMS delivery relative to each participant's baseline rate. An omnibus two-way ANOVA on the normalized discrimination rates, with rTMS Location (occipital, parietal, sham) and SOA (50, 100, 150 msec) as the two within-subject factors, revealed a significant main effect of SOA,  $F(2, 2) = 4.14$ ,  $p = .02$ , and a marginally significant interaction between rTMS and SOA conditions,  $F(2, 2) = 2.5$ ,  $p = .051$  (Figure 2A). The main effect of rTMS condition was not significant. To confirm that participants perceived both stimuli with the same overall accuracy and hence that our results cannot be explained by a systematic bias in the rate of report of one of the stimuli, we compared the discrimination rates for squares (mean rate = 81%) and diamonds (mean rate = 84%) between participants from all masked target trials, including no-rTMS catch trials. A two-sample *t* test revealed no significant difference between discrimination rates for the two stimuli,  $t(14) = 0.32$ ,  $p = .75$ .

To determine the source of these effects, we conducted pairwise comparisons between the target discrimination rates in the parietal condition and the two control conditions at each time point, as well as the rates at each rTMS condition between the 50 and 100 msec SOAs. After correcting for multiple comparisons using the Holm–Bonferroni method, two-tailed *t* tests revealed a significant pairwise difference only between the 50 and 100 msec SOAs in the parietal rTMS condition,  $t(7) = 4.50$ ,  $p = .025$ . There were no significant differences between the 50 and 150 msec or

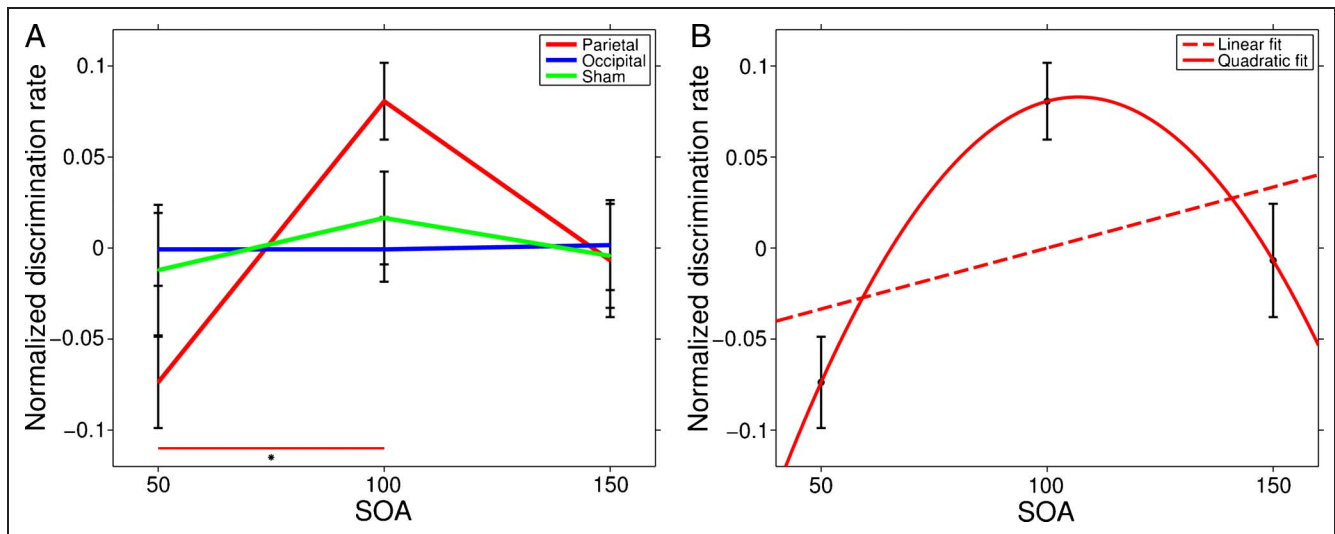


**Figure 2.** Results of the behavioral experiment. (A) rTMS of the parietal cortex at 50 msec before target onset impaired performance relative to baseline, whereas rTMS of the parietal cortex at 100 msec enhanced performance (horizontal red bar at graph bottom). Asterisk denotes pairwise significance at  $p < .05$ . (B) Best linear and quadratic fits for the discrimination results after parietal stimulation. A quadratic function offered the best fit of the data in the parietal condition. Occipital and sham best fits are not shown, as neither a linear fit nor a quadratic fit explained the data better than a horizontal line. Data from all target/mask-present trials with rTMS were included in our analysis (324 trials per participant). Error bars indicate *SEM*.

the 100 and 150 msec SOAs in the parietal condition, and no other comparisons of interest were significant after correcting for multiple comparisons. Furthermore, normalized discrimination rates were indistinguishable between occipital and sham conditions at all time points examined. These results suggest that the overall effect was driven by a decrease in discrimination in the parietal condition at 50 msec and an increase in discrimination in the parietal condition at 100 msec relative to baseline.

To confirm that the results were because of an oscillatory-like change in discrimination only in the parietal rTMS condition and to explicitly examine our hypothesis that perceptual discrimination accuracy after parietal rTMS increases and decreases following an alpha-like cycle, we found the best-fitting linear and quadratic curves for the behavioral data in each rTMS condition at the three SOAs. Curve goodness of fit, as measured by adjusted  $R^2$ , increased from the linear to the quadratic fit only in the case of the parietal data (linear fit: adjusted  $R^2(22) = 0.04$ , RMSE = 0.09; quadratic fit: adjusted  $R^2(21) = 0.40$ , RMSE = 0.07; Figure 2B). In both the occipital and sham conditions, goodness of fit worsened between the linear and quadratic fits, and in fact adjusted  $R^2$  was negative in all cases, indicating that both data sets are better fit by a horizontal line (occipital linear fit: adjusted  $R^2(22) = -0.05$ , RMSE = 0.06; occipital quadratic fit: adjusted  $R^2(21) = -0.09$ , RMSE = 0.06; sham linear fit: adjusted  $R^2(22) = -0.04$ , RMSE = 0.0845; sham quadratic fit: adjusted  $R^2(21) = -0.07$ , RMSE = 0.09). Our behavioral results indicate that the overall difference in participants' discrimination of masked targets was driven by a decrease at 50 msec, an increase at 100 msec, and a relative decrease at 150 msec after parietal rTMS delivery. Alpha rTMS over the parietal cortex thus appears to impair

or enhance visual target perception in an oscillatory-like manner at an alpha rhythm.

## EEG

During the behavioral task and rTMS procedure, we recorded scalp EEG to obtain an index of neural activity after each rTMS burst. Figure 3 (A, B) displays the average EEG activity across participants on all artifact-free rTMS trials in the alpha band (9–12 Hz) for the period after TMS artifact removal. To assess whether the phasic changes in visual discrimination after parietal rTMS are a consequence of induced phase changes in the alpha oscillation, we first extracted a continuous measure of the alpha-band ITC from the EEG recording in the period following the rTMS burst in each rTMS condition (Figure 3C, D). Because we only analyzed the data after the rTMS artifact, the ITC temporal resolution is limited in the period immediately following rTMS. Nonetheless, ITC is markedly higher in the parietal condition in the period immediately following rTMS, including the 50 msec SOA condition, at both the Oz and P2 electrodes. ITC as measured at the P2 electrode remained above chance in both the parietal and occipital rTMS conditions until after 150 msec, and the values at the Oz electrode largely remained above chance in both the parietal and occipital rTMS conditions over this same period. However, the coherence in the occipital rTMS condition did not reliably differ from the coherence in the sham rTMS condition in the period following the linear interpolation for artifact removal (35 msec post-rTMS), although both were above chance levels. The observed entrainment effects were not isolated to these electrodes, but rather extended to the electrodes over occipital and

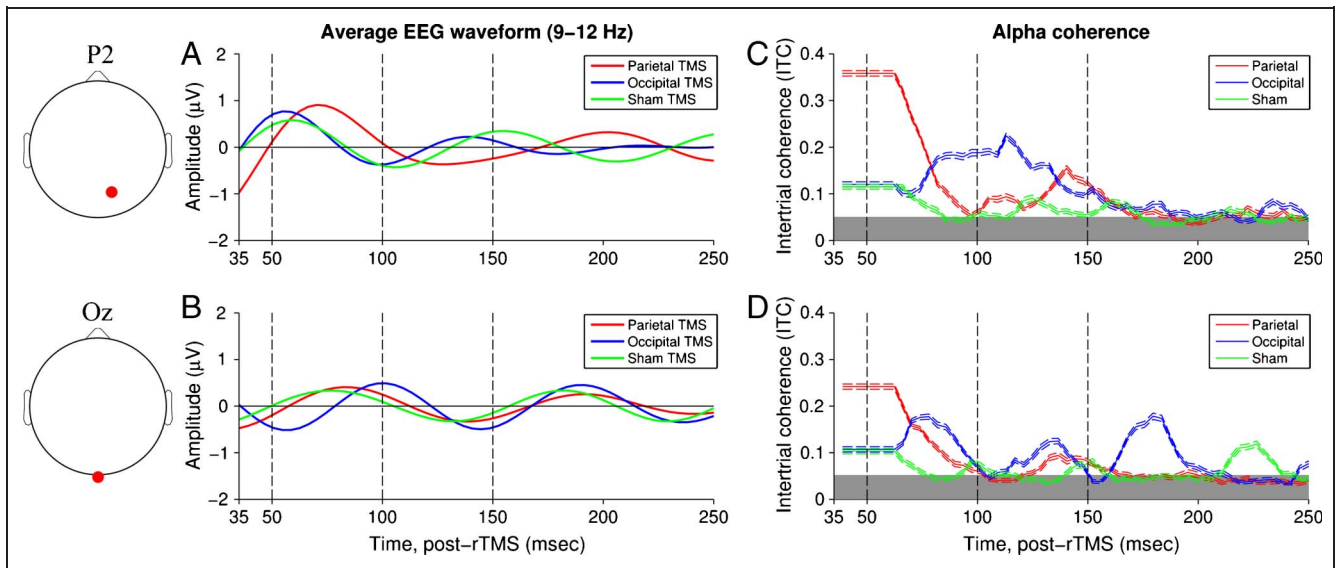
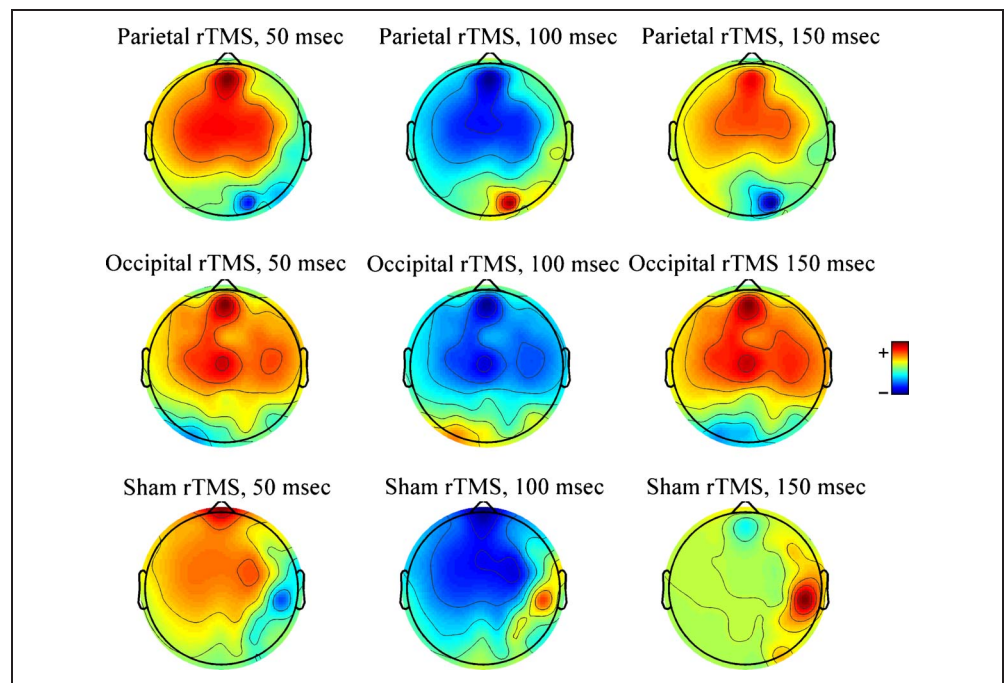


**Figure 3.** Average alpha-band EEG waveforms and continuous ITC values in each rTMS condition at times following artifact interpolation, measured at electrodes P2 (top row) and Oz (bottom row). All data are filtered with a bandpass FIR filter to include only frequencies in the alpha band (9–12 Hz). (A, B) Alpha-band waveforms are displayed for data after the period of artifact removal ending at 35 msec after the final TMS pulse. (C, D) Solid lines indicate the ITC values for each rTMS condition, and dashed lines indicate bootstrapped 95% confidence intervals (100 iterations). The gray field indicates the significance boundaries, with significance set at  $p < .01$ . The ITC estimates in the period immediately following the artifact are flat because of limited temporal resolution in the first wavelet cycle used to estimate coherence. Parietal rTMS produces the strongest coherence in the early post-stimulation period extending past 50 msec, as measured at both P2 and Oz electrodes. At the 150 msec SOA, phase coherence in the parietal condition is similar to that in the other two conditions. Data from all rTMS-present trials were included in our analyses (972 trials per participant).

**Figure 4.** Topographic maps of the alpha-band (9–12 Hz) EEG signal at the three times of interest following parietal, occipital, and sham rTMS. Scale bars represent the relative power of signal at an area in standardized units (red = strongest power). In all three conditions, regions of elevated power are distributed over occipital and parietal cortices. As expected, parietal and occipital rTMS trials exhibit hotspots at relatively parietal and occipital locations, respectively. One hotspot in the sham conditions appears to fall over parieto-temporal cortex, suggesting an influence of the auditory stimulus produced by TMS discharge on rTMS-alpha entrainment. In all three conditions, the measured signal appears to follow an alpha-like progression at individual hotspots, with minima and maxima separated by 50-msec intervals. Data from all rTMS-present trials were included in our analyses (972 trials per participant).



right parietal areas, as suggested by the broad occipito-parietal distribution of alpha effects after rTMS (Figure 4). In summary, alpha was entrained with a broad posterior distribution in both the parietal and occipital rTMS conditions for up to 150 msec post-rTMS, but parietal rTMS elicited the strongest effect at both the P2 and Oz electrodes in the early period following rTMS.

We next examined the specific phase of entrained alpha at the three SOAs. Rayleigh tests for nonuniformity

of the distribution of circular data revealed deviation from uniformity for the parietal rTMS condition at 50 and 100 msec, in the occipital condition at all three SOAs, in the sham condition at 50 msec (in all cases at  $p < .05$ ), as well as marginally significant deviation from uniformity in the parietal condition at 150 msec ( $p = .068$ ). All Rayleigh test  $p$  values are reported after adjustment for multiple comparisons using the Holm–Bonferroni method. Figure 5 shows these differences on circular histograms of

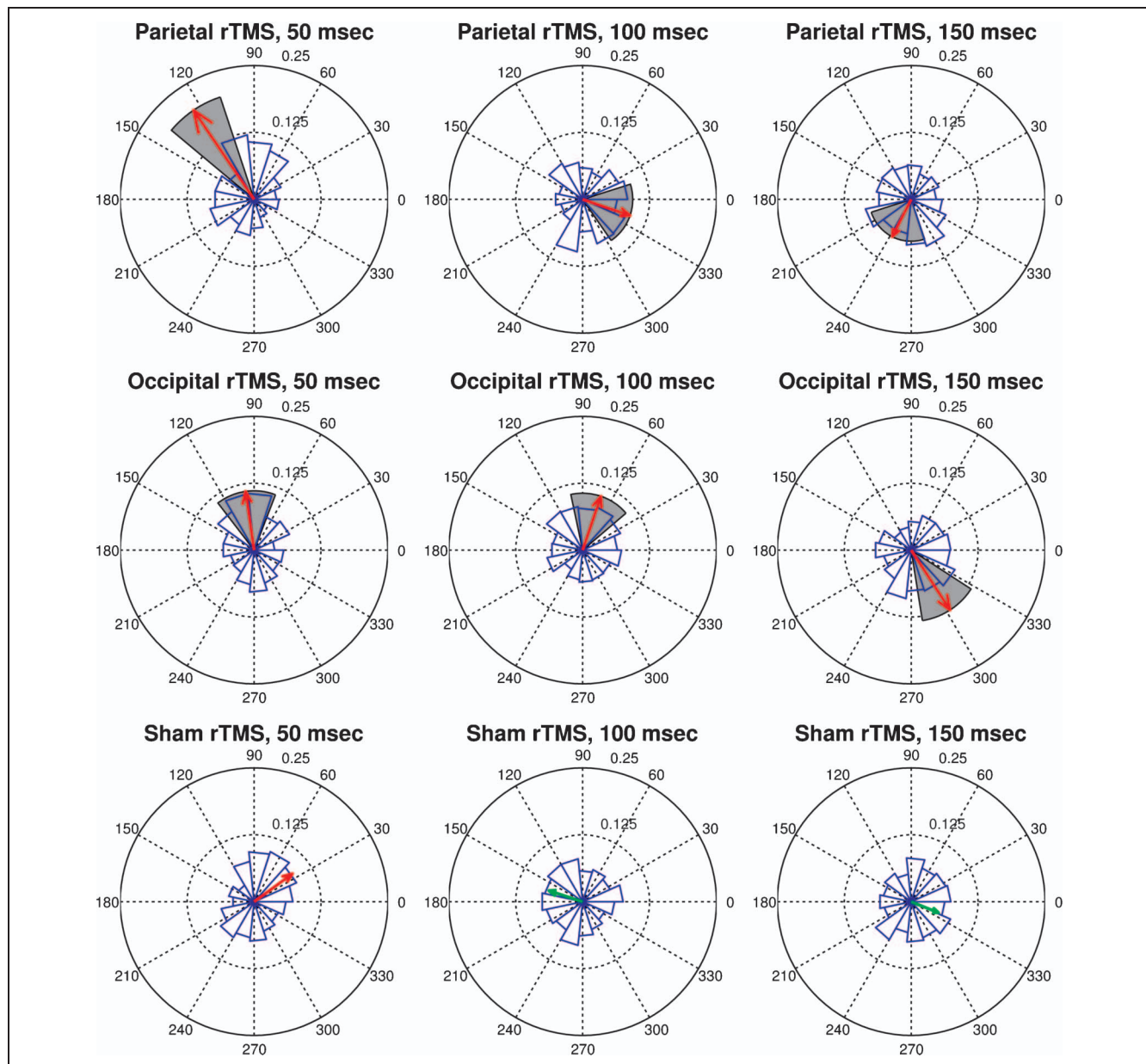


**Figure 5.** Circular histograms of instantaneous phase at 50, 100, and 150 msec after each rTMS condition, pooled across participants, trials, and SOA conditions at parietal electrode P2. The displayed mean resultant vector indicates the measured mean phase angle in each condition. The length of the vector is a measure of phase coherence, where a length of 0 indicates uniform phase distribution and a length of 1 indicates perfect coherence. Vectors are drawn in red if they represent significant deviation from uniformity (at  $p < .05$ ) and in green otherwise. In line with the discrimination performance results, note the opposite phase angles for the 50 and 100 msec SOA conditions following rTMS of the parietal cortex. 99% confidence intervals, determined by Kuiper’s test, are displayed in gray for parietal and occipital rTMS conditions. Confidence intervals could not be calculated for the sham condition because of the small probability of deviation from uniformity. Data from all rTMS-present trials were included in our analyses (972 trials per participant).

the distribution of phase angles across participants and trials, with the resultant circular mean in each condition displayed in red when significant deviation from uniformity occurred and in green when no significant deviation from uniformity occurred. In accordance with the ITC factors plotted in Figure 3, the strongest phase coherence occurs in the parietal condition at early SOAs.

If alpha phase directly influences discrimination performance, there should be a consistent sinusoidal phase progression after rTMS. For example, if the mean phase at one time point were  $0^\circ$ , the mean phase at a time point one half-period (50 msec) later should be  $180^\circ$ . To show that alpha-like phase progression occurred after parietal rTMS but not after occipital rTMS between the 50 and 100 msec time points, we ran a two-factor ( $2 \times 2$ ) Harrison–Kanji (H-K) test. The H-K test is an analogue of the ANOVA suitable for comparisons on circular data (Philipp, 2009). This test revealed a highly significant main effect of SOA and a highly significant SOA  $\times$  rTMS Position interaction (both at  $p < .001$ ), as well as a marginally significant main effect of rTMS Position ( $p = .08$ ).

The significant SOA and interaction effects of the H-K test were driven by the  $\sim 180^\circ$  phase shift between 50 and 100 msec SOAs in the parietal rTMS condition. To confirm that the means were in fact centered in opposing phase quadrants, we conducted one-sample Kuiper's tests for data in the parietal and occipital rTMS conditions at these times points. This statistical test (the circular analogue to the Kolmogorov–Smirnov test) evaluates whether phase distribution deviates from uniformity with a hypothesized mean direction (Mardia & Jupp, 1999). We found deviation from uniformity in the parietal rTMS conditions at 50 and 100 msec with mean phases centered at nearly opposite angles in opposite quadrants of the alpha waveform (at  $p < .01$ ). Thus, an rTMS-induced phase shift at alpha frequencies occurred between 50 and 100 msec in the parietal rTMS condition. In the occipital rTMS condition, Kuiper's test revealed probable means within the same phase quadrant at both 50 and 100 msec (at  $p < .01$ ). All Kuiper's test  $p$  values are reported after correcting for multiple comparisons using the Holm–Bonferroni method. We therefore conclude that no robust phase change occurred in the occipital rTMS condition between the 50 and 100 msec SOAs. The results of the H-K test and Kuiper's tests mirror the ANOVA and  $t$  tests of the behavioral data: The strongest and most consistent modulation occurred in the parietal rTMS condition between the 50 and 100 msec time points. This suggests that phase entrainment and progression in the parietal condition drives behavioral performance.

## DISCUSSION

Our results provide direct evidence that the phase of entrained alpha rhythms at the time of stimulus presentation causally controls the perception of that stimulus. Additionally, our data provide evidence that alpha can

be entrained in a phase-specific manner by rTMS to affect behavior. The behavioral changes that we differentially drive with phasic rTMS provide further evidence that stimuli presented at one phase of the alpha waveform are detected at a higher rate than stimuli presented at the opposite phase.

Furthermore, our results suggest a hierarchical role for certain areas and networks in the alpha perceptual/attentional system. We were unable to effectively entrain alpha phase with stimulation of occipital visual areas to the extent necessary to produce a behavioral change, even with the TMS intensity set at a level high enough to produce phosphenes. Occipital cortex itself thus seems to play a limited role in the direct generation of the endogenous alpha oscillation that affects visual perception. However, rTMS over parietal regions at the same intensity produced robust alpha entrainment throughout posterior regions. In particular, parietal rTMS appears to produce the largest entrainment in a short interval following rTMS. Entrainment after occipital rTMS is lower initially, but peaks with a delay before aligning with parietal entrainment (see Figure 3C and D). This delay in the peaks of entrainment following occipital stimulation (observed at both the Oz and P2 electrode sites) may reflect reverberating feedback from higher regions of the cerebral cortex that is driven by the initial rTMS perturbation of occipital sensory neurons. Although the delay in the peak is present at both occipital and parietal electrodes, it is more pronounced at Oz, as we would expect if this entrainment reflects the delayed propagation of a feedback signal from parietal to occipital areas. A similar delay in the peaks of activity is observed in the sham condition. Thus, the primary alpha-related effect of occipital and sham rTMS may be to entrain parietal cortex by means of the output of stimulated sensory neurons (either visual or auditory).

These results support the suggestion that parietal alpha generators play a role in driving alpha activity in lower visual or sensory areas. The delay in the peaks of alpha entrainment after the occipital and sham conditions may also explain the null behavioral results for those conditions. Top-down oscillatory activity arising from parietal cortex may serve as a mechanism for directing attention and regulating sensory neuron excitability (Mathewson et al., 2011). Indeed, other recent work suggests that the parietal alpha band may play an important role in setting the attentional state (Romei, Thut, Mok, Schyns, & Driver, 2012).

Occipital rTMS could have potentially contributed to the null behavioral effects observed in this condition by inducing the perception of phosphenes and distracting participants from accurately perceiving the target. Although we are unable to verify that participants did not see or were not distracted by phosphenes in this condition, none of the participants reported seeing or being distracted by phosphenes during the experiment. Two facets of our data also suggest that phosphene perception did not affect behavior following occipital rTMS. First, if phosphenes

were induced by rTMS, we should expect to see better behavioral performance at the later SOAs. However, there were no changes in performance between any of the occipital SOAs. Second, we did not observe an overall difference in performance between the occipital and either the parietal or sham rTMS conditions, which suggests that phosphenes did not produce an overall degradation in performance in the occipital rTMS condition. Therefore, we find it unlikely that phosphene induction could explain the results of the occipital rTMS condition.

The modest degree of phase coherence present in the sham condition may be due in part to rhythmic biasing independent of cortical stimulation, and rhythmic anticipation may contribute to the coherence in parietal and occipital conditions. Alpha reset has been shown to be produced by auditory stimulation alone (Romei, Gross, & Thut, 2012), so it is possible that the 10 Hz rhythmic clicking associated with rTMS contributes to the measured coherence. However, despite this measured coherence, the phase in the occipital rTMS condition does not progress in a consistent sinusoidal manner from 50 to 100 msec, and the coherence observed in the sham condition was minimal compared with the parietal and occipital conditions. This suggests that any bias because of auditory stimulation or entrainment from rTMS of occipital visual neurons at the intensities we used is not enough to overpower other sources of endogenous alpha, such as those coming from the unstimulated parietal cortices.

Our results thus suggest that alpha may principally act as a gating or gain control signal driven by parietal areas, rather than a purely sensory signal, and that the net gain control may be minimal at lower levels of phase coherence. Results from the literature suggest that a large enough sensory signal, driven either by an external sensory stimulus or by stimulation of sensory cortex, may be sufficient to reset alpha and produce alpha-dependent behavioral modulations (Neuling et al., 2012; Thut et al., 2012; Rohenkohl & Nobre, 2011; Mathewson, Fabiani, Gratton, Beck, & Lleras, 2010; Capotosto et al., 2009). The lack of behavioral effects after occipital stimulation in our experiment may be related to the intensity of the rTMS. We stimulated occipital cortex at phosphene threshold, and participants did not attend to the phosphenes, so this stimulation may have had minimal efficacy as an entrainer. A high level of alpha coherence, such as seen at early latencies following parietal stimulation, may be induced with higher intensities of occipital rTMS and may be necessary to produce a noticeable behavioral change and might be induced with higher intensities of occipital rTMS. Thus, although the mean occipital phase appears to shift 90° between 100 and 150 msec, the overall coherence may be too low for this to produce a net behavioral effect. This is consistent with earlier experiments suggesting that behavioral modulations follow alpha phase only at high alpha power (Mathewson et al., 2009).

We also note that all rTMS pulses in our experiment were delivered at 10 Hz and individual peak alpha frequencies often differ from 10 Hz, which may lessen the effect of 10 Hz stimulation. Accordingly, future studies using different stimulation frequencies, perhaps tailored to each individual's optimal frequency bands, would be informative regarding how other oscillation frequencies might contribute to visual perception. Perhaps because of the large rTMS artifact in our recordings and an insufficient number of trials per condition, we were unable to obtain reliable or meaningful temporal ITC and power estimates across a wide number of frequency bands in the period following rTMS. Previous studies examining oscillatory and entrainment influences on visual perception have demonstrated preferential effects in the alpha-band frequency range (e.g., Romei et al., 2010; Mathewson et al., 2009). However, other studies have demonstrated perceptual effects of entrainment in frequency bands other than alpha at brain regions and frequencies relevant to other perceptual tasks (Chanes, Quentin, Tallon-Baudry, & Valero-Cabré, 2013; Romei, Driver, Schyns, & Thut, 2011). Future studies should examine the phasic perceptual effects of occipito-parietal stimulation in other frequency bands to clarify the specific role played by alpha in these networks in modulating visual perception.

Our study also addresses the claim that alpha effects are merely correlative “resonance” effects caused by some intrinsic property of sensory neuronal networks and that they do not reflect a top-down oscillatory control mechanism (Klimesch, Sauseng, & Hanslmayr, 2007). Because bin-sorting studies of alpha do not induce alpha but rather sort trials by phase or power to examine behavioral patterns, they remain open to this purely correlative explanation. Resonance has been addressed in part by studies that examine phase-dependent effects time-locked to the presentation of visual or auditory stimuli (Mathewson et al., 2010, 2012; Romei, Gross, et al., 2012; Rohenkohl & Nobre, 2011). Such experiments have been able to demonstrate alpha-like behavioral outcomes synchronized with external sensory stimuli. These studies leave open the possibility that stimulus presentation resets an oscillation produced by resonance with an external rhythmic or anticipatory event. Such alpha-like resonance effects might emerge as a result of activity in some other neural system, leading to purely epiphenomenal phasic behavioral outcomes. To fully demonstrate that neural alpha oscillations are causally efficacious and not mere resonance effects, it is necessary not only to reset alpha and produce alpha-like behavioral changes, but also to do so specifically by means of the networks that produce endogenous alpha. By producing a phasic behavioral change with direct stimulation of posterior parietal cortex, one source of alpha oscillations, we offer strong evidence that alpha oscillations do not emerge as passive resonance but are instead generated in parietal networks to drive activity in lower sensory areas.

## Acknowledgments

We thank Nianci Lo for assistance with data collection. This research was supported by NSF grant BCS 0843148 to Tony Ro.

Reprint requests should be sent to Tony Ro, Department of Psychology, NAC 7/120, The City College of New York, 160 Convent Ave., New York, NY 10031, or via e-mail: tro@ccny.cuny.edu.

## REFERENCES

- Adrian, E. D., & Matthews, B. H. C. (1934). The Berger rhythm: Potential changes from the occipital lobes in man. *Brain*, *57*, 355–385.
- Başar, E. (2012). A review of alpha activity in integrative brain function: Fundamental physiology, sensory coding, cognition and pathology. *International Journal of Psychophysiology*, *86*, 1–24.
- Başar, E., & Güntekin, B. (2012). A short review of alpha activity in cognitive processes and in cognitive impairment. *International Journal of Psychophysiology*, *86*, 25–38.
- Berger, P. D. H. (1929). Über das Elektrenkephalogramm des Menschen. *Zeitschrift für die gesamte Neurologie und Psychiatrie*, *87*, 527–570.
- Bolognini, N., & Ro, T. (2010). Transcranial magnetic stimulation: Disrupting neural activity to alter and assess brain function. *Journal of Neuroscience*, *30*, 9647–9650.
- Busch, N. A., Dubois, J., & VanRullen, R. (2009). The phase of ongoing EEG oscillations predicts visual perception. *Journal of Neuroscience*, *29*, 7869–7876.
- Capotosto, P., Babiloni, C., Romani, G. L., & Corbetta, M. (2009). Frontoparietal cortex controls spatial attention through modulation of anticipatory alpha rhythms. *Journal of Neuroscience*, *29*, 5863–5872.
- Chanes, L., Quentin, R., Tallon-Baudry, C., & Valero-Cabré, A. (2013). Causal frequency-specific contributions of frontal spatiotemporal patterns induced by non-invasive neurostimulation to human visual performance. *Journal of Neuroscience*, *33*, 5000–5005.
- Delorme, A., & Makeig, S. (2004). EEGLAB: An open source toolbox for analysis of single-trial EEG dynamics including independent component analysis. *Journal of Neuroscience Methods*, *134*, 9–21.
- Dugué, L., Marque, P., & VanRullen, R. (2011). The phase of ongoing oscillations mediates the causal relation between brain excitation and visual perception. *Journal of Neuroscience*, *31*, 11889–11893.
- Haegens, S., Nacher, V., Luna, R., Romo, R., & Jensen, O. (2011).  $\alpha$ -Oscillations in the monkey sensorimotor network influence discrimination performance by rhythmic inhibition of neuronal spiking. *Proceedings of the National Academy of Sciences*, *108*, 19377–19382.
- Hanslmayr, S., Aslan, A., Staudigl, T., Klimesch, W., Herrmann, C. S., & Bäuml, K.-H. (2007). Prestimulus oscillations predict visual perception performance between and within subjects. *Neuroimage*, *37*, 1465–1473.
- Jensen, O., & Mazaheri, A. (2010). Shaping functional architecture by oscillatory alpha activity: Gating by inhibition. *Frontiers in Human Neuroscience*, *4*, 186.
- Klimesch, W. (2012).  $\alpha$ -Band oscillations, attention, and controlled access to stored information. *Trends in Cognitive Sciences*, *16*, 606–617.
- Klimesch, W., Sauseng, P., & Gerloff, C. (2003). Enhancing cognitive performance with repetitive transcranial magnetic stimulation at human individual alpha frequency. *European Journal of Neuroscience*, *17*, 1129–1133.
- Klimesch, W., Sauseng, P., & Hanslmayr, S. (2007). EEG alpha oscillations: The inhibition-timing hypothesis. *Brain Research Reviews*, *53*, 63–88.
- Lakatos, P., Karmos, G., Mehta, A. D., Ulbert, I., & Schroeder, C. E. (2008). Entrainment of neuronal oscillations as a mechanism of attentional selection. *Science*, *320*, 110–113.
- Lindsley, D. B. (1952). Psychological phenomena and the electroencephalogram. *Electroencephalography and Clinical Neurophysiology*, *4*, 443–456.
- Mardia, K. V., & Jupp, P. E. (1999). *Directional statistics*. London: Wiley.
- Mathewson, K. E., Fabiani, M., Gratton, G., Beck, D. M., & Lleras, A. (2010). Rescuing stimuli from invisibility: Inducing a momentary release from visual masking with pre-target entrainment. *Cognition*, *115*, 186–191.
- Mathewson, K. E., Gratton, G., Fabiani, M., Beck, D. M., & Ro, T. (2009). To see or not to see: Prestimulus  $\alpha$  phase predicts visual awareness. *Journal of Neuroscience*, *29*, 2725–2732.
- Mathewson, K. E., Lleras, A., Beck, D. M., Fabiani, M., Ro, T., & Gratton, G. (2011). Pulsed out of awareness: EEG alpha oscillations represent a pulsed-inhibition of ongoing cortical processing. *Frontiers in Psychology*, *2*, 99.
- Mathewson, K. E., Prudhomme, C., Fabiani, M., Beck, D. M., Lleras, A., & Gratton, G. (2012). Making waves in the stream of consciousness: Entraining oscillations in EEG alpha and fluctuations in visual awareness with rhythmic visual stimulation. *Journal of Cognitive Neuroscience*, *24*, 2321–2333.
- Neuling, T., Rach, S., Wagner, S., Wolters, C. H., & Herrmann, C. S. (2012). Good vibrations: Oscillatory phase shapes perception. *Neuroimage*, *63*, 771–778.
- Philipp, B. (2009). CircStat: A MATLAB toolbox for circular statistics. *Journal of Statistical Software*, *31*, 1–21. Retrieved from www.jstatsoft.org/v31/i10.
- Rohenkohl, G., & Nobre, A. C. (2011).  $\alpha$  Oscillations related to anticipatory attention follow temporal expectations. *Journal of Neuroscience*, *31*, 14076–14084.
- Romei, V., Brodbeck, V., Michel, C., Amedi, A., Pascual-Leone, A., & Thut, G. (2008). Spontaneous fluctuations in posterior  $\alpha$ -band EEG activity reflect variability in excitability of human visual areas. *Cerebral Cortex*, *18*, 2010–2018.
- Romei, V., Driver, J., Schyns, P. G., & Thut, G. (2011). Rhythmic TMS over parietal cortex links distinct brain frequencies to global versus local visual processing. *Current Biology*, *21*, 334–337.
- Romei, V., Gross, J., & Thut, G. (2010). On the role of prestimulus alpha rhythms over occipito-parietal areas in visual input regulation: Correlation or causation? *Journal of Neuroscience*, *30*, 8692–8697.
- Romei, V., Gross, J., & Thut, G. (2012). Sounds reset rhythms of visual cortex and corresponding human visual perception. *Current Biology*, *22*, 807–813.
- Romei, V., Thut, G., Mok, R. M., Schyns, P. G., & Driver, J. (2012). Causal implication by rhythmic transcranial magnetic stimulation of alpha frequency in feature-based local vs. global attention. *European Journal of Neuroscience*, *35*, 968–974.
- Sauseng, P., Klimesch, W., Heise, K. F., Gruber, W. R., Holz, E., Karim, A. A., et al. (2009). Brain oscillatory substrates of visual short-term memory capacity. *Current Biology*, *19*, 1846–1852.
- Scheeringa, R., Mazaheri, A., Bojak, I., Norris, D. G., & Kleinschmidt, A. (2011). Modulation of visually evoked cortical fMRI responses by phase of ongoing occipital alpha oscillations. *Journal of Neuroscience*, *31*, 3813–3820.

- Thut, G., & Miniussi, C. (2009). New insights into rhythmic brain activity from TMS-EEG studies. *Trends in Cognitive Sciences*, *13*, 182–189.
- Thut, G., Miniussi, C., & Gross, J. (2012). The functional importance of rhythmic activity in the brain. *Current Biology*, *22*, R658–R663.
- Thut, G., Veniero, D., Romei, V., Miniussi, C., Schyns, P., & Gross, J. (2011). Rhythmic TMS causes local entrainment of natural oscillatory signatures. *Current Biology*, *21*, 1176–1185.
- Varela, F. J., Toro, A., John, E. R., & Schwartz, E. L. (1981). Perceptual framing and cortical alpha rhythm. *Neuropsychologia*, *19*, 675–686.
- Weisz, N., Lüchinger, C., Thut, G., & Müller, N. (2012). Effects of individual alpha rTMS applied to the auditory cortex and its implications for the treatment of chronic tinnitus. *Human Brain Mapping*. doi:10.1002/hbm.22152.
- Worden, M. S., Foxe, J. J., Wang, N., & Simpson, G. V. (2000). Anticipatory biasing of visuospatial attention indexed by retinotopically specific alpha-band electroencephalography increases over occipital cortex. *Journal of Neuroscience*, *20*, RC63.
- Zaehle, T., Rach, S., & Herrmann, C. S. (2010). Transcranial alternating current stimulation enhances individual alpha activity in human EEG. *PLoS One*, *5*, e13766.